Review

α-Fetoprotein growth inhibitory peptides: Potential leads for cancer therapeutics

Gerald J. Mizejewski and Robert MacColl

Wadsworth Center, New York State Department of Health, Albany, NY

Abstract

α-Fetoprotein (AFP), known largely as a growth-promoting agent, also possesses a growth inhibitory motif recently identified as an occult epitopic segment of the molecule. This segment, a 34-amino acid stretch termed the growth inhibitory peptide (GIP), has been chemically synthesized, purified, and characterized. The purified 34-mer exhibits complex aggregation behaviors; initially, trimeric oligomers were formed that possess growth inhibitory activity in rodent uterine bioassays. These rodent growth assays have served as a prelude to the anticancer studies that followed. In solution, the trimers convert slowly to dimers containing intrapeptide disulfide bonds; such dimers are inactive in the antigrowth assays. Cysteine-to-alanine analogues of the GIP retain the antigrowth properties, while similar cysteine-to-glycine and cysteine-to-serine analogues demonstrate little, if any, growth regulatory activity. Chemical modifications of the cysteine residues also have little influence on the antigrowth activity of the GIP. Fragments of the 34-mer possess variable growth activities of their own, with an octamer from near the carboxyl terminus displaying estrogen-dependent antigrowth activity similar to that of the 34-mer. It was further observed that the GIP can bind both Zn^{2+} and Co^{2+}; the Co^{2+} peptide complex was shown to have a distorted tetrahedral symmetry, involving coordination of two cysteine and two histidine residues. The Zn^{2+}-GIP complex had antigrowth activity and did not form the intrapeptide disulfide bond characteristic of the free GIP in aqueous solution. The GIP was tested *in vitro* for anticancer activity and was found to suppress the growth in 38 of 60 human cancer cell lines, representing nine different cancer types. *In vivo* studies of the GIP, certain analogues, and its fragments revealed anticancer activities in both isograft and xenograft animal tumor transplants. Furthermore, the 2C → 2A replacement analogue was active against a breast tumor *in vivo* and *in vitro* and a prostate cancer *in vitro*. Thus, it is proposed that the GIP, its analogues, and its fragment peptides can potentially serve as lead compounds for cancer therapeutics. (Mol Cancer Ther. 2003;2:1243–1255)

Introduction

α-Fetoprotein (AFP), a major transport protein in the fetus, has long served as a serum marker in the clinical laboratory for both cancer and fetal defects (1–3). During the last decade, a multitude of studies have established AFP as a growth regulator during ontogenic growth and tumor progression (4–8). It is in fact this growth-modulating activity that distinguishes AFP from albumin, another blood protein carrier/transport molecule. Findings now support the concept that AFP is largely a growth-enhancing agent and that this activity is performed through a cyclic AMP-protein kinase A activation pathway (9, 11–14). However, growth is a process that requires fine-tuning, for both up-regulation and down-regulation, to operate correctly over a defined period or event, such as pregnancy and cancer. Although sustained growth of the fetus is required for full-term pregnancy to be achieved, the fetus will encounter situations that require periods of temporary or prolonged growth cessation, such as differentiation and prevention of organ/tissue overgrowth (12). Furthermore, the fetus may experience pulses of stress/shock insults in the microenvironment in both extracellular and intracellular fetal mileux. Thus, fetal growth in a tissue or an extracellular matrix location may require a temporary halt until fetal homeostasis is achieved and until compensated signal transduction pathways are reestablished. Such stress/shock encounters include extremes of osmolality, pH, oxygen tension, ischemia, osmotic pressure, anemia, anoxia, and excessively high ligand concentrations.

A hidden amino acid stretch on human AFP (HAFP), termed the growth inhibitory peptide (GIP) segment (chemical synthesis core batch P149), has been synthesized, purified, characterized, and assayed for biological activity (11). The GIP segment lies buried in a molecular crevice and can be exposed following a conformational change in HAFP (Fig. 1; 15). Full-length HAFP contains the concealed epitope in its third domain, which exhibits a proposed rotational hinge (Fig. 1; 15). Thus, the hidden segment is an amino acid stretch on AFP that can potentially be exposed by extreme ligand concentrations and possibly by stress/shock conditions during fetal development (11, 15).

The present review will demonstrate that the GIP segment provides an ideal molecular platform for use as

Received 6/11/03; revised 7/31/03; accepted 9/2/03.

The costs of publication of this article were defrayed in part by the payment of page charges. This article must therefore be hereby marked advertisement in accordance with 18 U.S.C. Section 1734 solely to indicate this fact.

Requests for Reprints: Gerald J. Mizejewski, Wadsworth Center, New York State Department of Health, P. O. Box 509, Albany, NY 12201. Phone: (518) 486-5900; Fax: (518) 457-7893. E-mail: Mizejew@wadsworth.org

an anticancer agent due to its propensity for inhibiting growth, the major preoccupation of cancer cells. This propensity of the GIP, certain analogues, and its fragments has provided the underpinning for utilization of these peptides in a series of cancer therapeutic studies that will be described. The biological, biochemical, and biophysical properties of the GIP molecule will also be surveyed. Finally, we will explore the potential utilization of the GIP for biomedical research in cancer therapeutics for use in molecular targeting.

Historical Background

The concept of a growth inhibitory property embodied within the primary structure of mammalian AFP (rodent and human) originated from a series of experiments

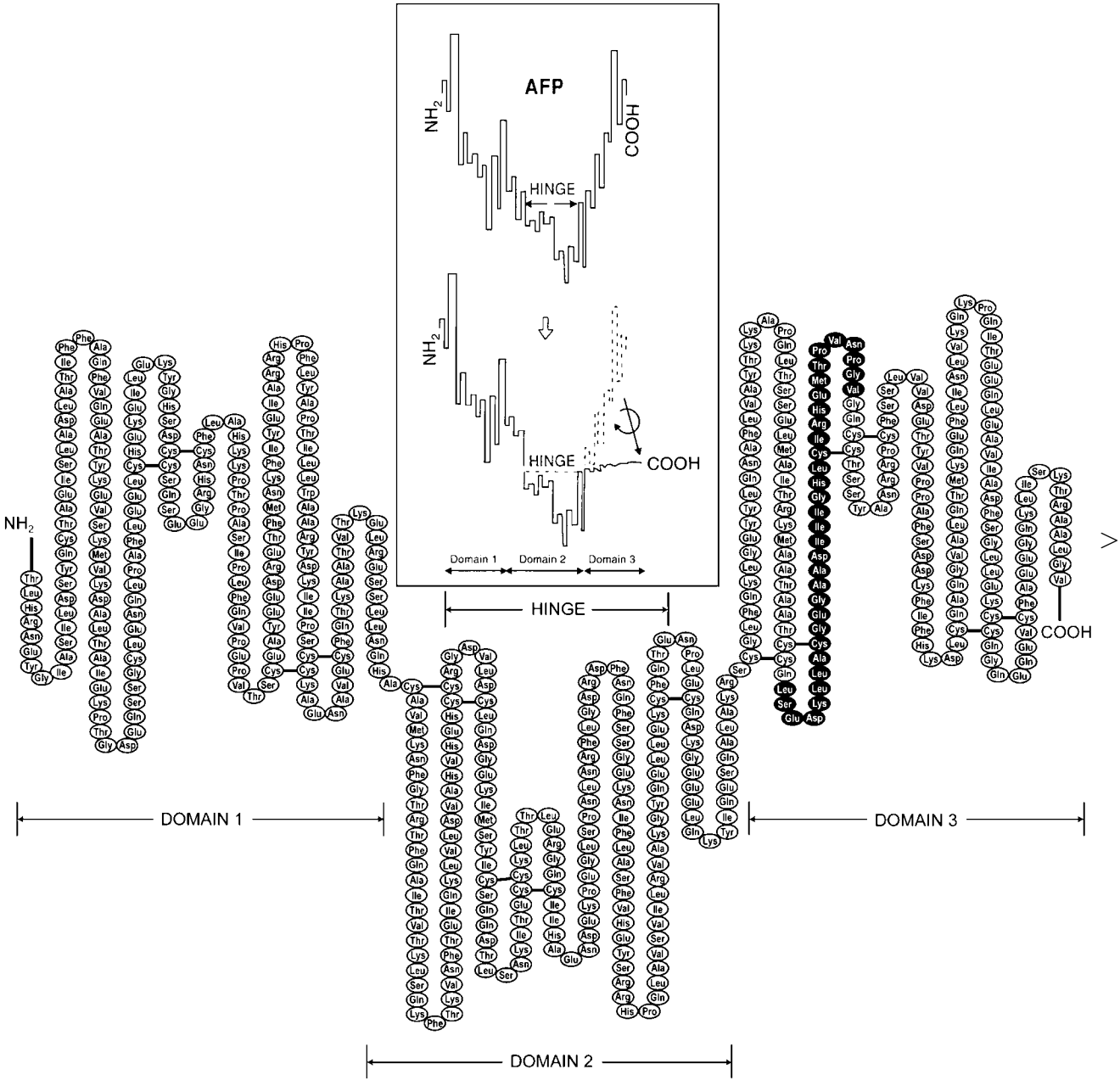

Figure 1. Primary and secondary structure amino acid sequence of HAFP. Note that the HAFP molecule is composed of three domains in a U-shaped configuration as confirmed by electron dot contour mass mapping. HAFP belongs to the albuminoid gene family, which is structurally characterized by cysteine residues that are folded into layers that form loops dictated by disulfide bridging (15). The GIP segment (*darkened circles*) is located and hidden on the third domain, positioned close to a proposed ''hinge'' region (see *arrows*). The hinge concept developed from the observation that HAFP has two disulfide bridges fewer than does human albumin, providing it with a means of molecular flexibility (82). Because the GIP segment is not detectable by conventional immunoassay procedures and can be exposed by high ligand concentrations (44), it is deemed an occult epitope.

performed in the early 1970s and 1980s (15–19). Prior investigations had employed anti-AFP antibodies as investigational probes to study the role of AFP in both ontogenic and oncogenic growth (17–21). It was from these anti-AFP antibody studies that the potential use of the AFP molecule in growth regulation was realized. When mouse AFP was used as a control for the antibody experiments, it was found that the fetal protein, incubated with estradiol (E2) in 130-fold molar excess, was capable of growth regulation in the prepuberal mouse uterus. From that initial observation, the growth regulatory properties of the AFP molecule were then investigatively pursued. The first demonstration of the antiuterotrophic action of the AFP-E2 complex was presented in a brief communication in 1982 (22) followed by a more detailed publication in 1983 (23). In that same year, the first report of an AFP-E2 complex-induced inhibition of rat mammary tumors appeared, demonstrating the specificity and sensitivity of the tumor growth suppression by purified full-length AFP incubated with E2 (24). Subsequent studies highlighting the growth regulatory (both antagonistic and potentiating) activities of mammalian AFP were then ongoing. During 1983–1985, reports detailed and documented use of the immature mouse uterine bioassay to measure and quantitate the inhibition of growth in normal tissues/organs (24, 25). At that same time, E2 addition/depletion experiments showed that minute amounts of AFP complexed with E2 were capable of blocking E2-supported growth of MTW9A breast tumors in rats (26). Further investigations revealed that AFP could regulate growth both in the normal immature uterus and in the adult ovariectomized mouse uterus (27). Later, it was documented that certain isoforms of mouse AFP were more susceptible to E2 transformation than were other isotypic variants (5).

From these observations, it was proposed that AFP might be present in adult cancer tissue as a means to regulate growth. This predicted location of AFP was borne out in experiments pursued by Sarcione and Hart (28) and Biddle and Sarcione (29) and later confirmed by Esteban *et al.* (30). Both a secreted and a nonsecreted form of AFP were detected in reproductive tissues (uterus and breast) and tumors (31, 32); however, their presence was not always as a free circulatory (immunoreactive) form but rather as a form bound to a protein (nonimmunoreactive; 32–34). In 1990, it was found that both mouse AFP and HAFP activated by complexing with E2 were capable of growth inhibition of MCF-7 human breast cancer xenografts (35). It was then demonstrated not only that AFP purified from human cord serum could be induced (via E2) to the activated growth regulatory form but also that some of the circulating AFP molecules were already present in an activated form during human pregnancy (36). During this period, an AFP ''cassette'' concept was proposed in which isolated stretches of amino acids on the AFP molecule were predicted to possess biological activities of their own (37, 38). This concept was experimentally verified in a study employing a 34-amino acid segment from the third domain of HAFP that was identified, chemically synthesized, and bioassayed as a disrupter of endocrine-associated growth in the rodent bioassay (11). Subsequent findings served to confirm that this amino acid stretch was an active site of E2 regulatory growth on the native AFP molecule. Studies in the latter 1990s confirmed that (1) the recombinant HAFP itself (and not a ligand) displayed the growth regulatory property (39), (2) the growth regulatory activity as found in cord serum was already present on HAFP purified from hepatoma cell culture supernatants (40), and (3) the recombinant third domain of HAFP did indeed contain the growth inhibitory site previously seen on the 34-mer synthetic peptide (41).

The GIP Segment

The GIP sequence of the 34-mer segment on HAFP had been discovered by GenBank amino acid sequence matching against known binding sites of heat shock proteins (HSP; *i.e.*, HSP-70 and HSP-90) on the mammalian estrogen receptor (ER; 42). Because both rodent AFP and ER bind E2 with high affinity, the amino acid sequences of the AFP-ER alignment revealed that a comparable HSP-70 site was located on HAFP (Table 1; 13). The HSP binding sites have been localized to the ligand-binding domain of the ER and are positioned on the carboxyl-terminal side of the DNA binding domain and the nuclear localization site, lying in juxtaposition to the major E2 binding pocket (43). The HSP-70 site on HAFP was likewise positioned adjacent and downstream of the E2 binding site present on rodent AFP. The 34-mer GIP, termed P149, was chemically synthesized and purified, and its physiochemical properties were characterized (11). Synthetic fragments of the 34-mer P149 have been designated as P149a (the amino-terminal 12 amino acids), P149b (the hydrophobic midpiece consisting of 14 amino acids), and P149c (an eight-amino acid peptide located near the carboxyl terminus; see Table 1). By the latter half of the 1990s, the 34-mer peptide (P149) and all of its fragments had been synthesized, purified, and bioassayed for their antigrowth and anticancer properties both *in vitro* and *in vivo* (44). These studies are described in greater detail in the following sections.

GIP Physiochemical Properties

The purified GIP derived from HAFP was characterized in a series of physiochemical steps. The initial biochemical studies of the 34-mer segment established that purification by C-18 reverse-phase high-performance liquid chromatography (HPLC) resulted in a peptide with a molecular mass of 3573 Da as determined by electrospray ionization mass spectroscopy (11). The molecular mass was that expected from the sequence and showed that the two cysteines were not oxidized. Subjection of the peptide to sequence analysis validated the amino acid positions.

Circular dichroism (CD) in the far-UV of the P149 peptide displayed a negative maximum at about 201 nm. Computer analysis of the CD spectrum indicated the presence of β-sheet and other ordered structures in approximate equal proportions, with the remaining forms composed of β-turns and a small contribution of α-helix (see below). Fourier infrared spectroscopy results for the peptide yielded strong signals in both Amide I (1628 cm^{-1})

Table 1. Matching of amino acid region 445–480 of HAFP with conserved amino acid sequences of HSP-related factors

Protein	Amino acid sequence no.[a]	Amino acid sequence
HAFP 149	445–480	L S E D K L L A C G E G A A D I I I G H L C I R H E M T P V N P G V
Subfragments of P149		|←—— P 1 4 9 a ——→|←—— P 1 4 9 b ——→|←P 1 4 9 c ——→|
Rattine HSP-70	1335–1347	I F F S P L L D C G E G
Pea (*Pisum sativum*) HSP-70	552–558	A X E E G X S Q E C I G K L C I Q H E
Petunia (*Petunia hybrida*) HSP-70	533–550	A E E E G G S X E C I G E L C L Q H E
Clover (*Trifolium repens*) HSP-70	22–39	A Q E E G X S K E L I G E L C L Q H E
Tobacco (*Oryza sativa*) HSP-70	455–471	V D E E K S G X E L I G E L C L Q H E
Yeast calmodulin	77,300–77,311	E L V N R I G Q L C I R L K
Human calrecticulin	1535–1547	I Q S I I V G H L G W F Q X
Murine protein disulfide isomerase	130–131	T A D G I V S H L K K Q A G
Human calcitonin	1535–1547	R K F G S T L L I C I R H S
O. sativa UDP-glucose glycosyltransferase	335–353	N K K G K L M X M M T P P S P G M

Note: The amino acid sequence of the GIP (amino acids 445–480) has been matched to HSP and associated factors derived from the GenBank, Swiss Prot, and PIR databases using GCG software employing FASTA sequence comparison (44). The FASTA program employs a Z-score statistical algorithm to demonstrate identity/similarity between amino acid sequences. For comparison between short peptide sequences (<40 amino acid), a word score of 1–2 is employed with a default limit set at 2.0 and above. With the word score set, an E-value of 1–10 is considered significant. The 34-mer GIP has been divided into three fragments based on the original chemical synthesis of P149; these are denoted P149a, P149b, and P149c. Note that the majority of matches involved P149b, with fewer for P149a and with P149c contributing few or none. Of particular interest are the GEG sequences, which appears as a variation with EEG in the various P149a matches and the GHL sequences that are compared with GKL, GHL, and GEL in the P149b matches.
[a]Genbank derived.

and Amide II (1540 cm^{-1}) bands. The Amide I band in this position demonstrated the presence of a large β-sheet structure for the peptide. For Amide II, β-sheets usually display bands between 1551 and 1540 cm^{-1} and such were observed. Computer modeling of P149 demonstrated a large β-structure, with the inclusion of several β-turns having minimal α-helix, while hydrophilicity/hydrophobicity plots indicated an overall hydrophilic molecule (Wisconsin GCG software). Finally, computational analysis via GCG software indicated an isoelectric point of pI = 4.7 for the GIP, similar to that found in full-length AFP.

In subsequent investigations, the 34-mer peptide was studied by gel filtration HPLC and was found to exhibit scomplex aggregation behaviors (45). Soon after

Table 2. Listing of the oligonomeric states of AFP-derived peptides and analogues to their biological activities in an antigrowth assay

Peptide tested	Oligomeric state	Molecular mass (Da)	Antigrowth assay (% inhibition)
C peptide, freshly solubilized	Trimer	3573.2	40
C peptide, trimer off column	Trimer	3572.4[b]	35
C peptide dimer off column	Dimer	3570.3[b]	6[c]
C peptide, large aggregates off column	Polymers (~150 peptides)	~550,000	0[c]
C peptide, oligomeric/polymeric mixture	Polymers plus trimers	NA	0[c]
C peptide, carboxyl-methylated cysteine	Monomer	3687.9	29
C peptide, carboxyl-amidated cysteine	Monomer	3639.6	31
A peptide, mutated cysteine to alanine	Trimer	3507.3[b]	37
G peptide, mutated/cysteine to glycine	Dimer	3479.7	17[c]
S peptide, mutated cysteine to serine	Dimer	3541.1	0[c]
C peptide complexed to Zn^{2+} ions	Trimer	3639.6	43

Note: ND, not determined. Data were extracted from Refs. (45–48). The oligomeric states of the peptides were determined by gel filtration HPLC in which the molecular masses were calculated by comparisons with the elution times of known compounds.
[a]C, cysteine; A, alanine; S, serine; G, glycine.
[b]Molecular mass of the peptide monomer in the oligomeric state.
[c]Not statistically significant.

Table 1. (*Continued*)

Protein	% Identity/ similarity	% Total
HAFP 149	100/0	100
Subfragments of P149		
Rattine HSP-70	50/15	65
Pea (*Pisum sativum*) HSP-70	50/28	78
Petunia (*Petunia hybrida*) HSP-70	50/22	72
Clover (*Trifolium repens*) HSP-70	50/14	64
Tobacco (*Oryza sativa*) HSP-70	50/14	64
Yeast calmodulin	44/0	44
Human calrecticulin	38/15	53
Murine protein disulfide isomerase	36/21	57
Human calcitonin	28/14	42
O. sativa UDP-glucose glycosyltransferase	42/35	77

solubilization, the peptide formed trimers; however, at high concentrations (8 mg/ml), the trimers clustered into large aggregates, each comprising about 150 peptide units (Table 2). At 0.2 mg/ml, the trimeric oligomers slowly dissociated to form dimers, and a small proportion of these associated into hexamers. Mass spectroscopy showed that the dimers contained an intrapeptide disulfide bond, while the trimers of GIP had free cysteines (46). The two cysteines were also derivatized to either 5-(2-aminoethyl)cysteine or 5-methylcysteine.

Physiochemical analysis of the cysteine (C)-containing 34-mer was carried out using three analogues in which the two cysteines were replaced by alanines (A peptide), glycines (G peptide), or serines (S peptide; 46). At low concentrations (0.2 mg/ml), the C and A peptides formed trimers while the G and S peptides formed dimers; however, at high concentrations, all peptides extensively aggregated (Table 2). All of these peptides, although differing in amino acid content, had almost identical secondary structure as determined by CD (Table 3). Unlike the high α-helix content of full-length AFP, the three peptide analogues and the C peptide displayed low amounts of α-helix (~10%) accompanied by nearly equal amounts of β-sheets/turns (35%/35%) and other structure (20%). At trifluoroethanol (TFE) concentrations of 20% and higher, the C, A, and G peptides were converted into highly helical structures (Table 3; 46). The TFE reagent has the ability to convert peptides into helical configurations if they possess the innate propensity for such a secondary structure. These data suggest that the original 34-mer may possibly be in a highly α-helical form when it occurs as an intrinsic sequence within the confines of the native AFP molecule.

In further studies, it was observed that both Zn^{2+} and Co^{2+} ions could bind to the C peptide. The spectra of the Co^{2+} peptide complexes showed that (1) two thiolate bonds were bound to the metal ion and (2) the metal ion-ligand complex had a distorted tetrahedral symmetry (Fig. 2; 47). The UV CD spectra of the Zn^{2+} and Co^{2+} peptide complexes revealed similar secondary structures. Finally, the peptide displayed secondary conformational flexibility following exposure to TFE (see above) and after incubation at 60°C.

Studies of the GIP with substituted amino acids were continued in combination with the metal ion binding described above. Investigations of another analogue, in which the two histidines were replaced by alanines in the C peptide, were then pursued (48). Histidine is an ideal candidate for metal ion binding because this amino acid is thought to participate together with cysteine in coordination with metal ion binding to proteins/peptides. It was subsequently demonstrated that Co^{2+} formed a complex with the C peptide but not with the histidine-to-alanine peptide. These data suggest that one or two histidines in the C peptide serve as ligands for Co^{2+} ion binding (Fig. 2). The histidine-to-alanine analogue further displayed intramolecular disulfide bond formation similar to that of the C peptide (47, 48). However, Zn^{2+} added to the histidine-to-alanine analogue peptide was able to abrogate the change in gel filtration elution profile as that was seen for the C peptide. Unlike the Zn^{2+} ions, which stopped the formation of the disulfide bonds, the Co^{2+} ions potentiated formation of these bonds.

The A peptide, unlike the GIP, cannot form an internal disulfide bond and remains a trimer indefinitely. Dimers can arise from two different sources: either from the primary sequence of the amino acid as in the peptides for which serines or glycines replaced cysteines or from

Table 3. Comparison of secondary structure components of AFP-derived peptides with and without the addition of TFE

Peptide tested	Secondary structure components (%)			
	α-helix	β-sheets	β-turns	Other
Without TFE				
C peptide	10.6	33.4	27.1	27.0
A peptide	9.2	33.5	28.0	28.0
G peptide	9.6	34.0	27.5	27.9
S peptide	10.3	34.1	27.5	29.1
HA peptide	9.0	35.0	ND	ND
Addition of 25% TFE				
C peptide	27.4	20.4	31.5	19.7
A peptide	32.8	14.8	27.3	24.8
G peptide	22.5	22.5	26.8	27.3
Addition of 50% TFE				
C peptide	31.7	17.6	29.0	20.7
A peptide	38.4	13.7	28.8	19.3
G peptide	27.1	18.7	29.8	23.9

Note the increase of α-helix and decrease of β-sheet component following TFE treatment.

Note: C peptide, cysteines intact; A peptide, cysteines replaced by alanines; G peptide, cysteines mutated to glycines; S peptide, cysteines mutated to serines; HA peptide, histidines replaced by alanines. Data were obtained from Refs. (45, 46).

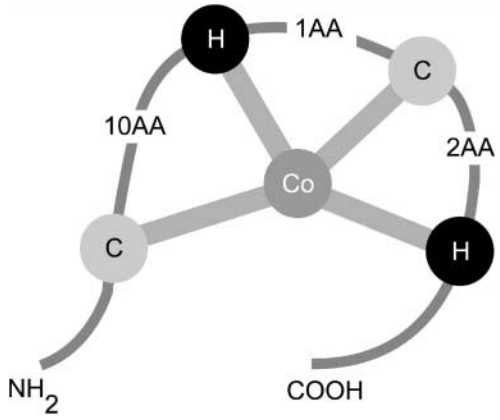

Figure 2. Schematic of the four amino acid ligands of GIP, two cysteines (*C*) and two histidines (*H*), which complex a Co^{2+} (*Co*) ion. The spectra of the Co^{2+} peptide binding showed that the complex has a distorted tetrahedral symmetry (see text).

internal disulfide bonding. Although both types of dimers have low activities in the rodent uterine assay, they have not been tested extensively in the anticancer assays.

Biological Activities

The GIP and Its Analogues: Antigrowth Properties

The C GIP peptide displayed considerable biological activity as an inhibitor of normal growth of the rodent uterus. The original report of GIP suppression of E2-dependent growth in the 24-h immature mouse uterus assay, with results published in 1996, showed an antiuterotrophic activity level of 40–50%; however, GIP was found to be incapable of inhibiting the water imbibition stage (4 h) of that 24-h uterotrophic response (11). A report followed in which both full-length AFP and the C peptide were demonstrated to inhibit the tail growth of thyroxine-induced tadpole metamorphosis, thus demonstrating a lack of species/class specificity for the antigrowth activity of GIP (49). Additional cross-species growth regulatory experiments were performed in chick embryos, demonstrating that the C peptide could also protect against insulin-induced congenital defects while producing growth-restricted chick fetuses (50). Finally, experimentation using estrogen fetotoxic doses in mouse embryos showed that the GIP could protect fetuses against hyperestrinism of pregnancy (50). These studies reinforced and confirmed the growth-suppressive properties originally ascribed to this AFP-derived peptide.

A series of physiochemical studies on GIP followed, comparing the oligomeric state of the C peptide to its antigrowth activity (see Ref. 45–48). For example, the complex aggregation behaviors of the various oligomers of the C peptide revealed that trimers were the active species in the uterine antigrowth assay, whereas both dimers and large aggregates were inactive (45). Carboxyl methylation

Table 4. Amino acid sequence matching of GIP peptide P149 with various seven-transmembrane domain G-coupled cell surface receptors

Protein name	Amino acid sequence matching
AFP peptide P149	L S E D K L L A C G B G A A D I I I G H L C I R H E M T P V N P G V G N
Fragments of P149	|←——— P149a ———→|←———— P 1 4 9 b ———→|←—— P149c ——→|
1 Human TGF-β	L S E D Q L L
2 Mouse prolactin receptor	L S E G K L L A
3 *Xenopus* acetylcholine (δ) receptor	L S G D K L L S
4 Human gastrin receptor	L S A D K L L
5 Mouse insulin growth factor-II receptor	E A R L L A C
6 *Drosophila* EGF receptor	A C G E G A E G N L L
7 Pig calcitonin	I I I V H L
8 Mouse T-cell receptor (BV)	C I R D N K T P
9 Human dopamine receptor	N P V D O G V G D
10 Human FKH protein	M T P V D P G V A Q
11 Mouse fibroblast growth factor receptor	E M T P A N P G
12 Rat somatostatin receptor	T T P I A P G V
13 Human homeprotein FKH	M T P V N P G V A Q
14 Rat glycine receptor tubulin linker	E M T P V L G T
15 Human T-cell CD2B	N M T P R R P G
16 Mouse insulin growth factor-II receptor	R M T P L T P P L

L S E D K L L, predicted internalization signal motif; consensus sequence X S/T X X R/K L L; P X X P, Src motif for protein-protein interaction; TGF, transforming growth factor; EGF, epidermal growth factor; FKH, forkhead.

The amino acid sequences of the GIP and its fragments (extending from 445 to 480) have been matched to various GPCRs and associated proteins using GCG-FASTA Software (see Fig. 2 legend). Most of the sequences were matched to the carboxyl terminus (P149c), fewer to the amino terminus (P149a), and the remainder fewest to the midpiece fragment (P149c).

and amidation modifications of the two cysteine residues of the C peptide also did not impair the antigrowth properties, suggesting that participation of the two free cysteines were not crucial for this activity (45).

Analogues produced by amino acid replacement showed that 2C → 2S substitutions resulted in peptides that were dimers and lacked the growth inhibitory activity for rodent uteri. However, the 2C → 2A analogues retained the trimer configuration and displayed substantial antigrowth properties (Table 2). In contrast, the 2C → 2G peptide assumed a dimeric state and displayed only marginal growth inhibitory capability. It was interesting that the secondary structures of the three analogues (A, G, and S) were found to be nearly identical, although the biological activity differed among the three peptides (Tables 2 and 5). A scrambled version of the C peptide was found to totally lack antigrowth activity (see Table 5).

The C peptide and its analogues were also studied to determine their metal binding properties. Zn^{2+} ions were found to bind to the 2C peptides, and the complex showed activity in the antigrowth assays; metal binding prevented formation of the biologically inactive forms (47). Co^{2+} also bound to the 2C peptide; surprisingly, it acted in reverse of the Zn^{2+} in that it catalyzed the formation of dimers and potentiated the loss of the antigrowth activity. Overall, data from the antigrowth assays revealed that complexing of Zn^{2+} to the C peptide maintained the peptides antigrowth property indefinitely in solution by protecting the peptide from undergoing disulfide bond formation.

Table 4. (*Continued*)

Protein name	% Identity/ similarity	% Total
AFP peptide P149	100/0	100
Fragments of P149		
1 Human TGF-β	86/0	86
2 Mouse prolactin receptor	86/0	86
3 *Xenopus* acetylcholine (δ) receptor	75/13	88
4 Human gastrin receptor	86/0	86
5 Mouse insulin growth factor-II receptor	71/14	85
6 *Drosophila* EGF receptor	55/18	73
7 Pig calcitonin	83/0	83
8 Mouse T-cell receptor (BV)	63/13	76
9 Human dopamine receptor	66/22	88
10 Human FKH protein	70/30	100
11 Mouse fibroblast growth factor receptor	88/0	88
12 Rat somatostatin receptor	63/25	88
13 Human homeprotein FKH	80/20	100
14 Rat glycine receptor tubulin linker	63/13	76
15 Human T-cell CD2B	63/13	76
16 Mouse insulin growth factor-II receptor	44/38	82

Peptide Fragments: Antigrowth Properties

Each of the three C peptide fragments (P149a, P149b, and P149c; see Table 1) was also chemically synthesized and then purified by reverse phase C-18 HPLC. While P149a and P149c are hydrophilic peptides, P149b is somewhat hydrophobic in aqueous solution. In a 1999 report (44), P149c was shown not only to suppress E2-stimulated uterine growth but also to inhibit growth in a mouse ascites mammary tumor. Additional studies of the P149c fragment have recently been reported (44, 51, 52). As discussed in these reports, P149c displayed robust antigrowth biological activity. Further studies demonstrated that cyclization of the P149c peptide produced activity in both the antigrowth and the anticancer assays of the octamer fragment (52). It is noteworthy that P149c inhibited E2-dependent, but not E2-independent, tumors in these studies (51, 52); however, the 34-mer suppressed the growth of both tumor types (see Table 3).

The antigrowth properties of the C peptide fragments (P149a, P149b, and P149c) have been documented (44). In that paper, it was demonstrated that a different antigrowth response was obtained for each fragment. For example, the uterine growth inhibition responses of P149a and P149c were 28% and 40%, respectively, while P149b showed only a marginal response at 20% in the mouse assay (45). In contrast, P149b tested in a rat bioassay showed a more pronounced uterine growth inhibition (see Table 5; 48). In addition, the 14-mer fragment of the C peptide, unlike the 34-mer C peptide, cannot form an internal disulfide bridge because it only contains one cysteine. The P149c fragment displayed an antiuterotrophic activity nearly identical to that of the 34-mer (P149). Other investigators confirmed that the antigrowth activity of P149c in a linear configuration (EMTPVNPG) was similar to that of the 34-mer (P149; 51). This latter group also reported that substitution of hydroxyproline for proline conserved the activity of the octamer peptide (52). Cyclization of the octamer peptide substantially broadened its effective dose range in the mouse uterine assay. Thus, both linear and cyclic versions of P149c appeared to be effective growth inhibitors.

Anticancer Activity

GIP: Anti-Oncogenic Properties

The initial report on the discovery of the estrogen regulatory (growth) segment on HAFP included studies of growth inhibition of MCF-7 human breast cancer cells *in vitro* (11). The C peptide inhibited the formation of foci formed as a result of the accumulation of breast cancer cells *in vitro*, which clump due to loss of contact inhibition (Table 6). The estrogen-induced focal growth suppression by the C peptide was extremely potent, displaying peak inhibitory doses at 10^{-12} to 10^{-10} M concentrations. Following that initial report, summary findings by the National Cancer Institute Therapeutics Drug Screening Program (Bethesda, MD) concerning the C peptide were issued (Table 7; 44). These findings described the *in vitro* results of the C peptide challenged against 60 different cell culture lines representing a variety of human cancers. In a

Table 5. Comparison of antigrowth and anticancer assays using AFP GIP P149 and its subfragments

Peptide tested	Antigrowth assay (% inhibition)		Anticancer assay (% inhibition)			
	Immature rodent uterine growth	Estrogen-induced fetotoxicity reduction	Human cancer cell lines (*in vitro*)		Isograft and xenograft tumors (*in vivo*)	
			Estrogen independent	Estrogen dependent	Estrogen independent	Estrogen dependent
C peptide P149	40 (M) 39 (R)	73	75[a]	70	65[b]	>75[a]
Subfragment P149a	30	63	50[c]	ND	(22)	ND
Subfragment P149b	20[d] (M) 45 (R)	67	15[c,d]	ND	31	ND
Subfragment P149c (linear)	43	37	30[a]	65[e]	39	>75[a]
Subfragment P149c (cyclic)	45	ND	ND	ND	0[f]	>80[a]
A peptide	34	ND	75[a]	ND	70	ND
G peptide	18[d]	ND	25	ND	60	ND
S peptide	0	ND	ND	ND	ND	ND
Scrambled peptide	0	0	0	0	0	0

Note: M, mouse assay; R, rat assay; 0, no activity. Estrogen fetotoxic assays were performed in prenatal mice. The estrogen-independent isograft is a mouse mammary acanthoma tumor. Data were obtained from Refs. (44–48, 51, 52).
[a]MCF-7 human breast cancer.
[b]GI-101 human ductal.
[c]Human kidney.
[d]Indicates lack of statistical significance for inhibition.
[e]T47D human breast cancer.
[f]MDA-MB-231 human breast cancer.

Table 6. Human and rodent breast tumors suppressed by GIP using *in vivo* and *in vitro* models

Tumor designation	Organism of origin	Cancer type	Receptor present	Morphology of tumor
MCF-7	Human	Glandular adenocarcinoma	Estrogen	Epithelial
T-47D	Human	Ductal carcinoma	Prolactin, progesterone, estrogen, androgen	Epithelial
BT-549	Human	Ductal papillary	Estrogen	Epithelial
MDA-MB-231	Human	Glandular adenocarcinoma	Epithelial	Wnt 7h Wnt 3
MDA-MB-435	Human	Glandular adenocarcinoma	EGF, TGF-α	Epithelial
GI-101, tamoxifen resistant	Human	Ductal carcinoma	EGF, estrogen pS2	Epithelial
EMT-6	Mouse	Mammary-derived sarcoma	EGF TGF-β	Spindle
6WI-1	Mouse	Adenoacanthoma	NR	Squamous (ascites adapted)
MCF-7 (foci assay)	Human	Glandular adenocarcinoma	Estrogen	Epithelial foci (overgrowth)
MCF-7 mouse xenograft	Human	Glandular adenocarcinoma	Estrogen	Estrogen[a] dependent (epithelial)

Note: NR, not reported; CC, cell culture; Wnt, wingless *Drosophila* homologue; acanthoma, adenoid squamous cell carcinoma; UD, unpublished data (G.J. Mizejewski and E. J. Sarcione).
[a]Estrogen pellets applied.

6-day proliferation assay, the P149 peptide was deemed cytostatic, not cytotoxic, against 38 of 60 cancer cell lines, representing nine different cancer cell types including prostate, breast, and ovarian cancers (Table 7). In the following year, the effective use of the C peptide and its fragments against various breast cancers was described (see Table 6). The anticancer activity of P149 peptide in a mouse mammary isograft was demonstrated by the peptide's suppression of 70% of the cell growth and 60% of the ascites fluid accumulation as compared with use of the vehicle control (Table 6; 44). As shown in the antigrowth assay above, a scrambled sequence version of the GIP totally lacked anticancer activity (see Table 5).

GIP: Anti-Breast Cancer Studies

The GIP was used in a myriad of studies involving breast cancer cells both *in vivo* and *in vitro* (Table 6; 44). As stated above, the C peptide had suppressed estrogen-supported formation of foci by 65–70% in breast cancer at 10^{-10} to 10^{-12} M concentrations of peptide (11). The peptide further inhibited the growth of human ductal breast cancer GI-101 cells, a non-estrogen-dependent tamoxifen-resistant carcinoma grown as a xenograft in nude mice (53). In cell culture cytostatic growth assays utilizing sulforhodomine staining, the GIP suppressed by 50–80% the growth of five different human breast cancer cell lines maintained in non-estrogen-supplemented growth media, thus demonstrating estrogen-independent growth. Finally, in a 60-day timed release pellet study (0.5 μg peptide/day), GIP suppressed the *in vivo* growth of the GI-101 ductal breast tamoxifen-resistant cancer cells by 70% (53) while MCF-7 human breast cancer was suppressed as xenografts in nude mice by GIP implant pellets with a release rate of 0.25 μg peptide/day (Table 6).

GIP Analogues: Anticancer Activities

Analogues of the C peptide substituting two alanines for the two cysteines were also subjected to anticancer studies. The A peptide was tested *in vitro* in two human cancer cell lines for evaluation of its antitumor activity (53). In investigation of MCF-7 breast cancer and LNCap prostate cancer cell lines, the A peptide was determined to be active against both tumor types, displaying >70% growth inhibition. A scrambled control peptide achieved <10% suppression in these cancer lines. The A peptide analogue was also found to display anticancer activity *in vivo* in a serially transplanted 6WI-1 mouse mammary tumor isograft (44). When the A peptide was given 1.0-μg daily doses throughout the post-transplantation period (12 days), a 60–70% reduction in both tumor cell proliferation and ascites fluid production was observed. Thus, the anticancer effects of the A peptide are seen in both cell culture and animal models.

The P149c Fragment: E2-Dependent Breast Cancer Studies

The eight-amino acid peptide (P149c) was also employed for studies of E2-dependent MCF-7 breast cancer cells both *in vivo* and *in vitro* (44, 51, 52). The octapeptide was shown to suppress E2-dependent breast cancer growth (in T47D cells) as previously reported for the 34-mer peptide and

Table 6. (*Continued*)

Oncogenes detected	Model type	Treatment duration (days)	Optimal concentration (M)	% Growth suppression	Reference
Wnt 7h	*In vitro* (CC)	6	10^{-7}	80	(44, 58)
Wnt 7h	*In vitro* (CC)	6	10^{-5}	25	(44, 58)
NR	*In vitro* (CC)	6	10^{-6}	40	(44, 58)
In vitro (CC)	6	10^{-7}	80	(59, 60)	
Wnt 7h Wnt 3	*In vitro*	6	10^{-7}	70	(44, 58)
Neu	*In vivo*	65	0.5 μg/day[b]	75	(53)
	In vitro	6	10^{-12}	88	(53)
NR	*In vivo*	28	None	0	(44, 53)
NR	*In vivo*	12	1–10.0 μg/day	47	(44, 58)
Wnt 7h	*In vitro* (CC)	14	10^{-10}	65	(11, 58)
Wnt 7h	*In vivo*	60	25 μg/day[a]	>80	UD

[b]Time release peptide pellets.

Table 7. The growth-suppressive (cytostatic) screening results of HAFP-derived peptide (P149) for multiple types of human tumor cell cultures

Human tissue of origin	Cell line designation	Tumor tissue type[a]	Concentration range (M)	% Inhibition	Growth response
Colon	KM-12	AC	10^{-5} to 10^{-7}	75	Suppression
	HCC-299	AC	10^{-5}, 10^{-7}	80	Suppression
	Colo-205	AC	10^{-5}	10	Slight suppression
	HCT-116	AC	10^{-5} to 10^{-7}	75	Suppression
Ovary	OVCAR-3	AC	10^{-5} to 10^{-7}	80	Suppression
	SK-OV-3	AC	10^{-5} to 10^{-7}	60	Suppression
	IGROV1	AC	10^{-5} to 10^{-7}	75	Suppression
	OVCAR-4	AC	10^{-5} to 10^{-7}	85	Suppression
Breast	MCF-7	AC	10^{-5} to 10^{-7}	80	Suppression
	MDA-MB-231	AC	10^{-7} only	80	Suppression
	MDA-MB-435	AC	10^{-5} to 10^{-7}	70	Suppression
	BT-549	AC	10^{-6} to 10^{-7}	25–40	Moderate suppression
	T-47D	AC	10^{-5}	25	Slight suppression
Prostate	PC-3	AC	10^{-6} to 10^{-7}	80	Suppression
	DU-145	AC	10^{-5} to 10^{-7}	90	Suppression
Non-small cell lung	HOP-62	CA	10^{-5} to 10^{-7}	75	Suppression
	NCI-H226	CA	10^{-5}	5–10	Slight suppression
	NCI-H460	CA	10^{-5} to 10^{-7}	80	Suppression
Melanoma	UACC-62	Epithelial	10^{-4} to 10^{-7}	80	Suppression
	SK-MeL-28	Squamous	10^{-4} to 10^{-7}	35	Mild suppression
	SK-MeL-5	Squamous	10^{-5}	10	Slight suppression
	SK-MeL-2	Squamous	10^{-5} to 10^{-7}	50–75	Moderate suppression
	UACC-257	Squamous	10^{-5} to 10^{-7}	75–80	Suppression
Central nervous system	SF-295	CA	10^{-5} to 10^{-7}	80	Suppression
	SF-539	CA	10^{-5}	15–20	Slight suppression
	U-251	CA	10^{-6} to 10^{-7}	45	Moderate suppression
	SNB-75	CA	10^{-6} to 10^{-7}	50	Moderate suppression
Kidney	TK-10	Renal CA	10^{-4} to 10^{-7}	85	Suppression
	RXF-393	Renal CA	10^{-6} to 10^{-7}	45–50	Moderate suppression
	A498	Renal CA	10^{-4} to 10^{-7}	75	Suppression
	ACHN	Renal CA	10^{-7} to 10^{-7}	80	Suppression
	CAK-1	Renal CA	10^{-5} to 10^{-7}	50–75	Moderate suppression
White blood cell	K-562	Leukemia	10^{-7}	45	Moderate suppression
	Molt-4	Leukemia	NA	10–15	Slight suppression
	SR	Leukemia	10^{-7}	25	Slight suppression
	RPMI-8236	Leukemia	10^{-6} to 10^{-7}	15–25	Slight suppression
	CCRF-CEM	Leukemia	10^{-5}	5–10	Slight suppression
	HL60-TC	Leukemia	10^{-5}	5–10	Slight suppression

Note: National Cancer Institute Therapeutics Drug Screening Program used with permission. Cells were exposed to the peptide for 6 days, fixed, and stained with sulforhodamine-β. All cell lines were not dependent on estrogen for growth.
[a]AC, adenocarcinoma; CA, carcinoma.

full-length AFP (51). Furthermore, both the linear and the cyclic octamers (P149c, also known as P472) inhibited the estrogen-dependent growth of the MCF-7 cells implanted in severe combined immunodeficient mice (51). A hydroxyproline-substituted analogue also completely prevented the xenograft growth of tamoxifen-resistant sublines of MCF-7 but was not able to suppress the growth of E2-independent cell line MDA-MB-231 human breast cancer (53, 54). Interestingly, the octamer peptide was further reported to inhibit the uterotrophic effect of tamoxifen in the mouse host following tumor transplantation (54). Thus, the octamer provided a two-pronged therapeutic attack: it inhibited tamoxifen-resistant breast cancer while suppressing the uterotrophic side effect of the tamoxifen. It is interesting that both linear and cyclic octamers are active only against E2-dependent breast cancer growth, whereas the C peptide is active against both E2-dependent and E2-independent growth (Table 6); this suggests a different mechanism of action for the latter. The tamoxifen studies suggest three exciting potential uses for these peptides. First, the octamers should be tested as replacements for tamoxifen; such a substitution would eliminate the side effects of uterine cancer and blood clotting. Second, the peptides could be used to supplement tamoxifen treatment. Third, they could be employed to treat tamoxifen-resistant cases.

Mechanism of Action

Data accumulated since 1993 have provided sufficient information for the emergence of a mechanism of action for GIP. For example, inhibition of the estrogen-induced

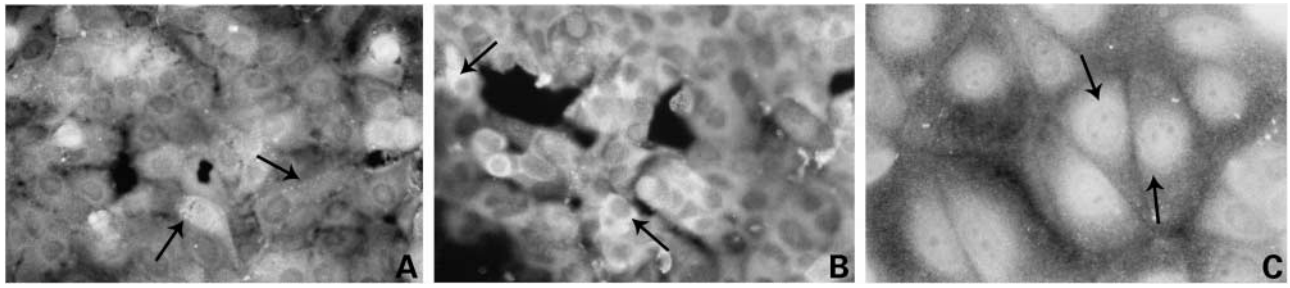

Figure 3. A three-panel photomicrograph of GIP binding and uptake in MCF-7 cells. Using the indirect immunofluorescence technique (fluoroscein-FITC), GIP was cytologically localized in three cellular compartments by means of pulse-chase experiments. **A,** GIP bound to the surface of the cells (*arrows*), within 5 min of exposure, in a punctuate, granular fashion; **B,** GIP was detected in the cell cytoplasm (*arrows*), within 1 h, in a diffuse, glowing distribution; **C,** GIP was observed at higher magnification in a perinuclear pattern (*arrows*) with fluorescence condensed around the nucleus by 3–4 h.

growth of the immature mouse uterus can be totally abrogated by prior injection of anti-GIP antibodies (11), suggesting a cell surface event. GenBank amino acid sequence matching (Table 4) suggests that GIP shares identity/similarity to multiple growth factors and receptors of the G-coupled protein gene families (Table 4). In fact, GIP was found to inhibit human chorionic gonadotropin-induced ovarian cell stimulation and corticosteroid stimulation of splenic growth, both G-protein-coupled receptor (GPCR) events (55, 56). A recent study of the P149c cyclic octamer, using computer modeling, lends further credence to the concept that GPCRs (*i.e.*, the GPCR 30) might be involved (57). Furthermore, the lack of cytotoxic activity and the demonstration of cytostatic effects on multiple tumor cell types (Table 7) suggest a nontoxic regulatory mechanism such as observed in the homologous/heterologous desensitization of GPCRs. In the process of GPCR desensitization, receptors are normally withdrawn from the cell surface due to overstimulation and are either recycled or subjected to lysosomal/proteosomal degradation. Finally, pulse-chase uptake experiments of GIP in cultured MCF-7 breast cancer cells have demonstrated that GIP binds to the cell surface within 5 min of exposure, is transcytosed to cytoplasm within 1 h, and can be observed in a perinuclear position by 3–4 h (Fig. 3 A–C).

It can be proposed, based on the above data and observations, that GIP might bind to an unknown GPCR in which the peptide serves as a decoy (and/or antagonist) ligand. Binding to the GPCRs with subsequent receptor occupancy induces receptor clustering and oligomerization of homologous and/or heterologous GPCRs. If GIP acts as a decoy ligand for the GPCR, it would mean that the GIP could bind to the extracellular loops of the GPCR but would not induce the conformational change necessary for activation of the receptor. This conformational change is related to an ionic lock between extracellular loops 2 and 3 and transmembrane domains 3 and 6 (58). If the ionic constraints are not released by the conformational change, then the receptor is unable to interact with the second phase, which is α-G-protein release. When a peptide ligand (serving as an agonist) normally binds to the GPCR, the receptor is phosphorylated when the α-G-protein component is released from the heterotrimeric α/βγ complex as a result of the GTP to GDP conversion. Arrestins then bind to the phosphorylated receptors and terminate signaling by interdicting receptor interaction with the G-proteins and promoting receptor internalization. Arrestins serve as a scaffold that links the phosphorylated signal substrates to the mitogen-activated protein kinase (MAPK) cascades. If GIP does indeed serve as a decoy ligand to induce receptor blockade, the GPCR will not be phosphorylated, arrestins will fail to bind to the receptors, and the MAPK cascade steps will not be linked and cell division (mitosis) would not occur; hence, cell growth would be suppressed. In this regard, AFP-derived peptides have been observed to down-regulate MAPKs (J. A. Bennett, unpublished observations).

Concluding Remarks

The AFP-derived 34-mer peptide and its three fragments have been demonstrated to suppress both ontogenic and oncogenic growth in cell culture and various animal models. These peptides could serve as ideal candidates for templates or lead compounds toward the development of anticancer drugs because efficacy has already been demonstrated. Because the peptides act on various proliferating tissues and a multitude of cancer types, the peptides could potentially provide site-directed targeted drug delivery to a variety of different types of cancer. Small organic mimics could be modeled to the P149 peptide and its fragments to provide second-generation drugs with oral modes of delivery. Finally, the AFP-derived peptides could find utility in the identification of molecular targets for drugs intended as biomodulation cancer therapies and to provide ''proof of concept'' in identifying targets for future peptide mimics (58).

Acknowledgments

We thank Drs. James Dias, Charles Hauer, Sam Bowser, Angelo Lobo, and Li-Ming Changchien, James Seeger, and Leslie Eisele of the Core Facilities of the Wadsworth Center for the expert preparations, characterization, purification, and analysis of the peptides, Dr. George Butterstein, Union College, Schenectady, NY, for research collaboration, our manuscript coauthors, and Lynda M. Jury for her commitment and time expenditure in the excellent typing and processing of the manuscript, references, and tables of this report.

References

1. Tatarinov, Y. S. Content of embryo-specific α-globulin in the blood serum of the human fetus, newborn, and adult man in primary cancer of the liver. Vop. Khim. SSR, *11:* 20 – 24, 1965.

2. Abelev, G. I. α-Fetoprotein in association with malignant tumors. Adv. Cancer Res., *14:* 295 – 357, 1971.

3. Mizejewski, G. J. New insights into AFP structure and function: potential biomedical applications. *In:* G. J. Mizejewski and I. H. Porter (eds.). α-Fetoprotein and Congenital Disorders, pp. 5 – 34. Orlando: Academic Press, 1985.

4. Toder, V., Blank, M., Gold-Gefter, L., and Nebel, J. The effect of α-fetoprotein on the growth of placental cells *in vitro*. Placenta, *4:* 79 – 86, 1983.

5. Mizejewski, G. J., Keenan, J. F., and Setty, R. P. Separation of the estrogen-activated growth regulatory forms of α-fetoprotein in mouse amniotic fluid. Biol. Reprod., *42:* 887 – 898, 1990.

6. Dudich, E., Semenkova, L., Gorbatova, E., Dudich, I., Khromykh, L., Tatulov, E., Grechko, G., and Sukhikh, G. Growth-regulative activity of human α-fetoprotein for different types of tumor and normal cells. Tumor Biol., *19:* 30 – 40, 1998.

7. Jacobson, H. I., Bennett, J. A., and Mizejewski, G. J. Inhibition of estrogen-dependent breast cancer growth by a reaction product of α-fetoprotein and estradiol. Cancer Res., *50:* 415 – 420, 1990.

8. Wang, X. W. and Xie, H. Stimulation of tumor cell growth by α-fetoprotein. Int. J. Cancer, *75:* 596 – 599, 1998.

9. Li, M. S., Li, P. F., Yang, F. Y., He, S. P., Du, G. G., and Li, G. The intracellular mechanism of AFP promoting the proliferation of NIH 393 cells. Cell Res., *12:* 151 – 156, 2002.

10. Mizejewski, G. J. α-Fetoprotein as a biologic response modifier: relevance to domain and subdomain structure. Proc. Soc. Exp. Biol. Med., *215:* 333 – 362, 1997.

11. Mizejewski, G. J., Dias, J. A., Hauer, C. R., Henrikson, K. P., and Gierthy, J. α-Fetoprotein derived synthetic peptides: assay of an estrogen-modifying regulatory segment. Mol. Cell. Endocrinol., *118:* 15 – 23, 1996.

12. Everman, D. B., Shuman, C., and Dzolganovski, B. Serum AFP levels in Beckwith-Wiedeman syndrome. J. Pediatr., *137:* 123 – 127, 2000.

13. Morinaga, T., Sakai, M., Wegmann, T. G., and Tomoaki, T. Primary structures of human AFP and its mRNA. Proc. Natl. Acad. Sci. USA, *80:* 4604 – 4608, 1983.

14. Mizejewski, G. J., Vonnegut, M., and Simon, R. Neonatal androgenization using antibodies to α-fetoprotein. Brain Res., *118:* 273 – 277, 1980.

15. Mizejewski, G. J. α Fetoprotein structure and function: relevance to isoform, epitopes, and conformation variants. Exp. Biol. Med., *226:* 377 – 408, 2001.

16. Mizejewski, G. J. and Vonnegut, M. Characterizations of the androgenization produced in mice by neonatal exposure to α-fetoprotein antibodies. Terotology, *25:* 351 – 360, 1982.

17. Mizejewski, G. J. and Allen, R. P. Immunotherapeutic suppression in transplantable solid tumors. Nature (Lond.), *250:* 50 – 52, 1974.

18. Mizejewski, G. J., Young, S. R., and Allen, R. P. α-Fetoprotein: effect of heterologous antiserum on hepatoma cells *in vitro*. J. Natl. Cancer Inst., *54:* 1361 – 1367, 1975.

19. Mizejewski, G. J. and Grimley, P. M. Abortogenic activity of antiserum to α-fetoprotein. Nature (Lond.), *259:* 222 – 224, 1976.

20. Mizejewski, G. J. and Allen, R. P. α-Fetoprotein: studies of tumor associated antigen cytotoxicity in mouse hepatoma BW7756. Clin. Immunol. Immunopathol., *11:* 307 – 317, 1978.

21. Mizejewski, G. J. and Dillon, W. R. Immunobiologic studies in hepatoma-bearing mice passively immunized to α-fetoprotein. Arch. Immunol. Exp. Ther., *27:* 655 – 662, 1979.

22. Jacobson, H. I. and Mizejewski, G. J. The anti-uterotrophic action of the α-fetoprotein-estradiol complex. Endocrinology, *110:* 302, 1982.

23. Mizejewski, G. J., Vonnegut, M., and Jacobson, H. I. Estradiol-activated α-fetoprotein suppresses the uterotrophic response to estrogens. Proc. Natl. Acad. Sci. USA, *80:* 2733 – 2737, 1983.

24. Jacobson, H. I. and Mizejewski, G. J. Effect of estradiol-activated α-fetoprotein on the growth of rat mammary tumors. Int. Assoc. Breast Tumor Res. Abstr., 34, p. 40, 1983.

25. Mizejewski, G. J., Vonnegut, M., and Jacobson, H. I. Studies of the intrinsic antiuterotrophic activity of murine α-fetoprotein. Tumor Biol., *7:* 19 – 28, 1986.

26. Jacobson, H. I. and Mizejewski, G. J. Estrogen-supported growth of MTW9A breast tumors in rats in blocked by minute amounts of AFP. *In:* G. J. Mizejewski and I. Porter (eds.). α-Fetoprotein and Congenital Disorders, pp. 337 – 338. New York: Academic Press, 1985.

27. Mizejewski, G. J. and Warner, A. S. α-Fetoprotein can regulate growth in the immature and adult hypophysectomized mouse uterus. J. Reprod. Fertil., *85:* 177 – 185, 1988.

28. Sarcione, E. J. and Hart, D. Biosynthesis of α-fetoprotein by MCF-7 human breast cancer cell. Int. J. Cancer, *35:* 315 – 318, 1985.

29. Biddle, W. and Sarcione, E. J. Specific cytoplasmic AFP binding protein in MCF-7 human breast cancer cells and primary breast cancer tissue. Breast Cancer Res. Treat., *10:* 279 – 286, 1987.

30. Esteban, C., Terrier, P., Frayssinet, C., and Uriel, J. Expression of the α-fetoprotein gene in human breast cancer. Tumor Biol., *17:* 299 – 305, 1996.

31. Sarcione, E. J. and Smalley, J. R. Intracellular synthesis of α-fetoprotein and fibrinogen without secretion by Zajdela rat hepatoma cells. Cancer Res., *36:* 3203 – 3205, 1976.

32. Smalley, J. R. and Sarcione, E. J. Synthesis of α-fetoprotein by immature rat uterus. Biochem. Biophys. Res. Commun., *92:* 1429 – 1434, 1980.

33. Sarcione, E. J., Zlotty, M., Delluomo, D. S., Mizejewski, G. J., and Jacobson, H. I. Detection and measurement of α-fetoprotein in human breast cancer cytosol after treatment with 0.4 M potassium chloride. Cancer Res., *43:* 37399 – 3741, 1983.

34. Sarcione, E. J. and Biddle, W. Elevated serum α-fetoprotein levels in postmenopausal women with primary breast carcinoma. Dis. Markers, *5:* 75 – 79, 1987.

35. Jacobson, H. I., Bennett, J. A., and Mizejewski, G. J. Inhibition of estrogen-dependent breast cancer growth by a reaction product of α-fetoprotein and estradiol. Cancer Res., *50:* 415 – 420, 1990.

36. Allen, S. H. G., Bennett, J. A., Mizejewski, G. J., Andersen, T. T., Ferraris, S. P., and Jacobson, H. I. Purification of α-fetoprotein from human cord serum with antiestrogenic activity. Biochem. Biophys. Acta, *1202:* 135 – 142, 1993.

37. Mizejewski, G. J. An apparent dimerization motif in the third domain of α-fetoprotein: molecular mimicry of the steroid/thyroid nuclear receptor superfamily. Bioessays, *15:* 427 – 432, 1993.

38. Dauphinee, M. J. and Mizejewski, G. J. Human α-fetoprotein contains potential heterodimerization motifs capable of interaction with nuclear receptors and transcription/growth factors. Med. Hypotheses, *58:* 453 – 461, 2002.

39. Bennett, J. A., Semeniuk, D. J., Jacobson, H. I., and Murgita, R. A. Similarity between natural and recombinant human AFP as inhibitors of estrogen-dependent breast cancer growth. Breast Cancer Res. Treat., *45:* 169 – 179, 1997.

40. Bennett, J. A., Zhu, S., Pogano-Mirachi, A., Kellom, T. A., and Jacobson, H. I. AFP derived from a human hepatoma, prevents growth of estrogen-dependent human breast cancer xenografts. Clin. Cancer Res., *4:* 2877 – 2884, 1998.

41. Festin, S. M., Bennett, J. A., Fletcher, P. W., Jacobson, H. I., Shaye, D. D., and Andersen, T. T. The recombinant third domain of human α-fetoprotein retains the antiestrotrophic activity found in the full length molecule. Biochem. Biophys. Acta, *24789:* 307 – 314, 1999.

42. Spannjaard, R. A., Darling, D. S., and Chin, W. W. Ligand binding and heterodimerization activities of a conserved region in the ligand-binding domain of thyroid receptor. Proc. Natl. Acad. Sci., *88:* 8587 – 8591, 1991.

43. Wurtz, J. M., Bourguet, W., Renaud, J. P., Vivat, V., Chambon, P., Moras, D., and Gronemeyer, H. A canonical structure for the ligand-binding domain of nuclear receptors. Nat. Struct. Biol., *3:* 87 – 94, 1996.

44. Vakharia, D. and Mizejewski, G. J. Human α-fetoprotein peptides bind estrogen receptor and estradiol and suppress breast cancer. Breast Cancer Res. Treat., *63:* 41 – 52, 2000.

45. Eisele, L. E., Mesfin, F. B., Bennett, J. A., Andersen, T. T., Jacobson, H. I., Soldwedel, H., MacColl, R., and Mizejewski, G. J. Studies on a growth-inhibitory peptide derived from α-fetoprotein and some analogs. J. Peptide Res., *57:* 29 – 38, 2001.

46. Eisele, L. E., Mesfin, F. B., Bennett, J. A., Andersen, T. T., Jacobson, H. I., Vakharia, D. D., MacColl, R., and Mizejewski, G. J. Studies on analogs of a peptide derived from α-fetoprotein having anti-growth properties. J. Peptide Res., *57:* 539 – 546, 2001.

47. MacColl, R., Eisele, L. E., Stack, R. F., Hauer, C., Vakharia, D. D.,

Bennett, A., Kelly, W. C., and Mizejewski, G. J. Interrelationships among secondary structure, and metal ion binding for a chemically synthesized 34-amino acid peptide derived from α-fetoprotein. Biochem. Biophys. Acta, *1528:* 127–134, 2001.

48. Butterstein, G., MacColl, R., Mizejewski, G. J., Eisele, L. E., and Meservey, J. Biophysical studies and anti-growth activities of a peptide, a certain analog, and a fragment peptide derived from AFP. J. Peptide Res., *61:* 1–6, 2003.

49. Butterstein, G. M. and Mizejewski, G. J. α-Fetoprotein inhibits frog metamorphosis: implications for protein motif conservation. Comp. Biochem. Physiol., *124A:* 39–45, 1999.

50. Butterstein, G. M., Morrison, J., and Mizejewski, G. J. Effect of α-fetoprotein and derived peptides on insulin- and estrogen-induced fetotoxicity. Fetal Diag. Ther., *125:* 1080–1089, 2003.

51. Mesfin, F. B., Bennett, J. A., Jacobson, H. I., Zhu, S., and Andersen, T. T. α-Fetoprotein derived antiestrotrophic octapeptide. Biochim. Biophys. Acta, *1501:* 33–43, 2000.

52. Mesfin, F. B., Andersen, T. T., Jacobson, H. I., Zhu, S., and Bennett, J. A. Development of a synthetic cyclized peptide derived from AFP that prevents the growth of human breast cancer. J. Peptide Res., *58:* 246–256, 2001.

53. Caceres, G., Dauphinee, M. J., Eisele, L. E., MacColl, R., and Mizejewski, G. J. Anti-prostate and anti-breast cancer activities of two peptides derived from α-fetoprotein. Anticancer Res., *22:* 2817–2820, 2002.

54. Bennett, J. A., Mesfin, F. B., Andersen, T. T., Gierthy, J. F., and Jacobson, H. I. A peptide derived from α-fetoprotein prevents the growth of estrogen-dependent human breast cancers sensitive and resistant to tamoxifen. Proc. Natl. Acad. Sci. USA, *99:* 2211–2215, 2002.

55. Mizejewski, G. J. Growth inhibitory peptide. United States Patent 5,674,842, U.S. Patent Office Filing US00567 4842A, Oct. 7, 1997.

56. Mizejewski, G. J. Methods of using growth inhibitory peptides. United States Patent 5,707,963, U.S. Patent Office Filing US005707 963A, Jan. 13, 1998.

57. Hamza, A., Sarma, M. H., and Sarma, R. H. Plausible interaction of an α-fetoprotein cyclopeptide with the G-protein-coupled receptor model GPR30: docking study by molecular dynamics stimulated annealing. J. Biomol. Struct. Dyn., *20:* 751–758, 2003.

58. Mizejewski, G. J. Biological role of AFP in cancer: prospects for anticancer therapy. Exp. Rev. Anticancer Ther., *2:* 709–735, 2002.